

Collaborative SLAM for Facilitating Radiological Search and Mapping on UWB Enabled Multi-Agent Platforms

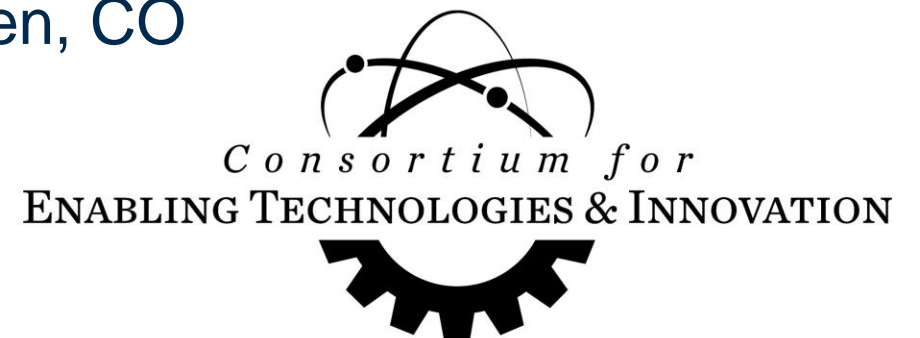
Andrew Fishberg

Jonathan P. How

Massachusetts Institute of Technology

ETI Annual Workshop

February 20 – 21, 2024, Golden, CO



Goal: Discuss the Results my Recent Paper



arXiv:2312.17731v1 [cs.RO] 29 Dec 2023

MURP: Multi-Agent Ultra-Wideband Relative Pose Estimation with Constrained Communications in 3D Environments

Andrew Fishberg Brian Quiter Jonathan P. How

Abstract—Inter-agent relative localization is critical for many multi-robot systems operating in the absence of external positioning infrastructure or prior environmental knowledge. We propose a novel inter-agent relative 3D pose estimation system where each participating agent is equipped with several ultra-wideband (UWB) ranging tags. Prior work typically supplements noisy UWB range measurements with additional *continuously* transmitted data, such as odometry, leading to potential scaling issues with increased team size and/or decreased communication network capability. By equipping each agent with multiple UWB antennas, our approach addresses these concerns by using only *locally* collected UWB range measurements, *a priori* state constraints, and detections of when said constraints are violated. Leveraging our learned mean ranging bias correction, we gain a 19% positional error improvement giving us experimental mean absolute position and heading errors of 0.24m and 9.5° respectively. When compared to other state-of-the-art approaches, our work demonstrates improved performance over similar systems, while remaining competitive with methods that have significantly higher communication costs. Additionally, we make our datasets available.

I. INTRODUCTION

Multi-robot systems can be used to improve the efficiency and robustness of large-scale tasks such as search & rescue [1], warehouse automation [2], and planetary exploration [3]. To operate and parallelize effectively, these systems typically need to know where the agent (and its peers) are located in a common reference frame. In practice this is often achieved by localizing within an *a priori* map or using an external measurement system like GPS or motion capture (mocap) [4], [5]. If these technologies are unavailable or infeasible, common approaches utilize both relative localization [6] and multi-agent SLAM [7] techniques.

Within the last decade, ultra-wideband (UWB) has matured into a reliable, inexpensive, and commercially available RF solution for data transmission, relative ranging, and localization – UWB now comes as standard issue in many popular smartphone devices [8]. For robotics, UWB has several properties of note: precision of approximately 10cm, ranges up to 100m, resilience to multipath, operates in non-line of sight (NLOS) conditions, low power consumption, and 100Mbit/s communication speeds [9]. Recent devices even extend the recommended and operational ranges to 300m and 500m respectively [10]. Nevertheless, UWB measurements are not immune from ranging errors or noise (see Section III-A), the modeling and correction of which is an active area of research [11]–[14].

* Work supported in part by DOE, NNSA, and ALB funding. A. Fishberg and J. How are with MIT Department of Aeronautics and Astronautics, {fishberg, jhow}@mit.edu. B. Quiter is with Lawrence Berkeley National Laboratory, bqquiter@lbl.gov.

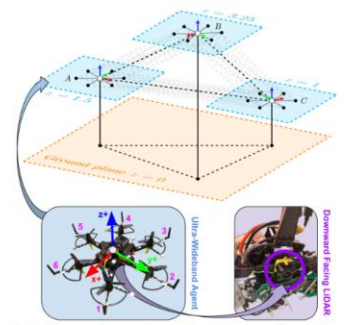


Fig. 1: Diagram of proposed system. Here three agents fly at different altitudes while performing real-time 3D relative pose estimation. Each agent is equipped with six ultra-wideband (UWB) antennas, each capable of performing pairwise relative ranging between all other agents' individual antennas. By using trilateration, an improved sensor model, and *a priori* state constraints about altitude/roll/pitch, agents can perform *instantaneous* estimation entirely with *locally* collected UWB measurements (i.e., without the need to *continuously* transmit other measurements, such as odometry). Additionally, each agent *locally* monitors its *a priori* constraints via downward facing LiDAR and IMU, and thus only needs to transmit *one-off* messages with the swarm if these assumptions change or are violated.

A common approach in UWB relative localization work fuses noisy UWB ranging measurements with additional *continuously* transmitted data, such as odometry [15] and visual inter-agent tracks [16], [17]. While these approaches achieve low absolute position error (APE) and absolute heading error (AHE), there are two prevalent shortcomings: (1) They often use a simplistic UWB measurement noise model (i.e., zero mean Gaussian), which then requires the use of supplementary measurements to compensate. (2) Reliance on these supplementary measurements (often *not locally*¹ collected, e.g., odometry), mandates their *continuous* transmission between agents, potentially impacting scalability to increased swarm size or decreased communication throughput.

Our previous work [18] used UWB to demonstrate an *instantaneous*² multi-tag approach to relative 2D pose estimation that achieved superior mean position accuracy and competitive performance on other metrics to Cao et al. [15]

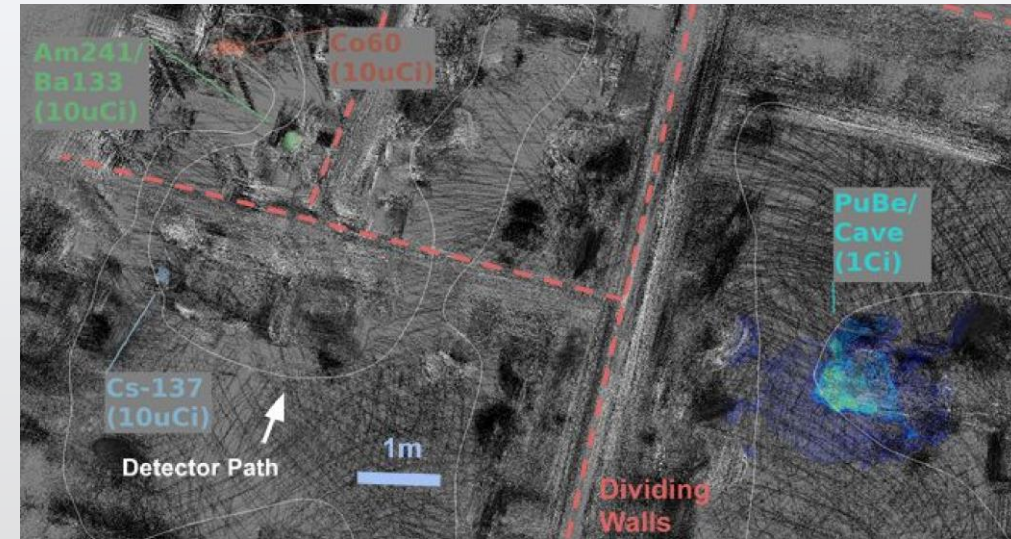
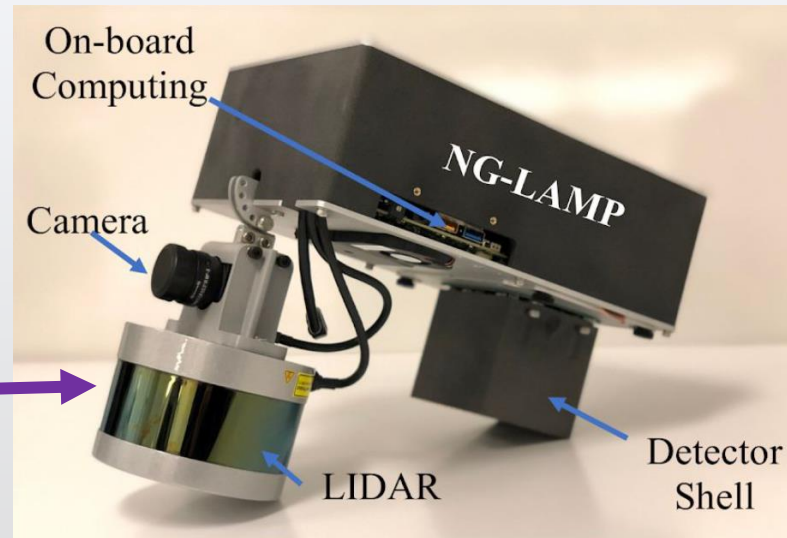


MURP: Multi-Agent Ultra-Wideband Relative Pose Estimation with Constrained Communications in 3D Environments
Being sent to IEEE's RA-L; Posted to arXiv December 2023

MOTIVATION & BACKGROUND

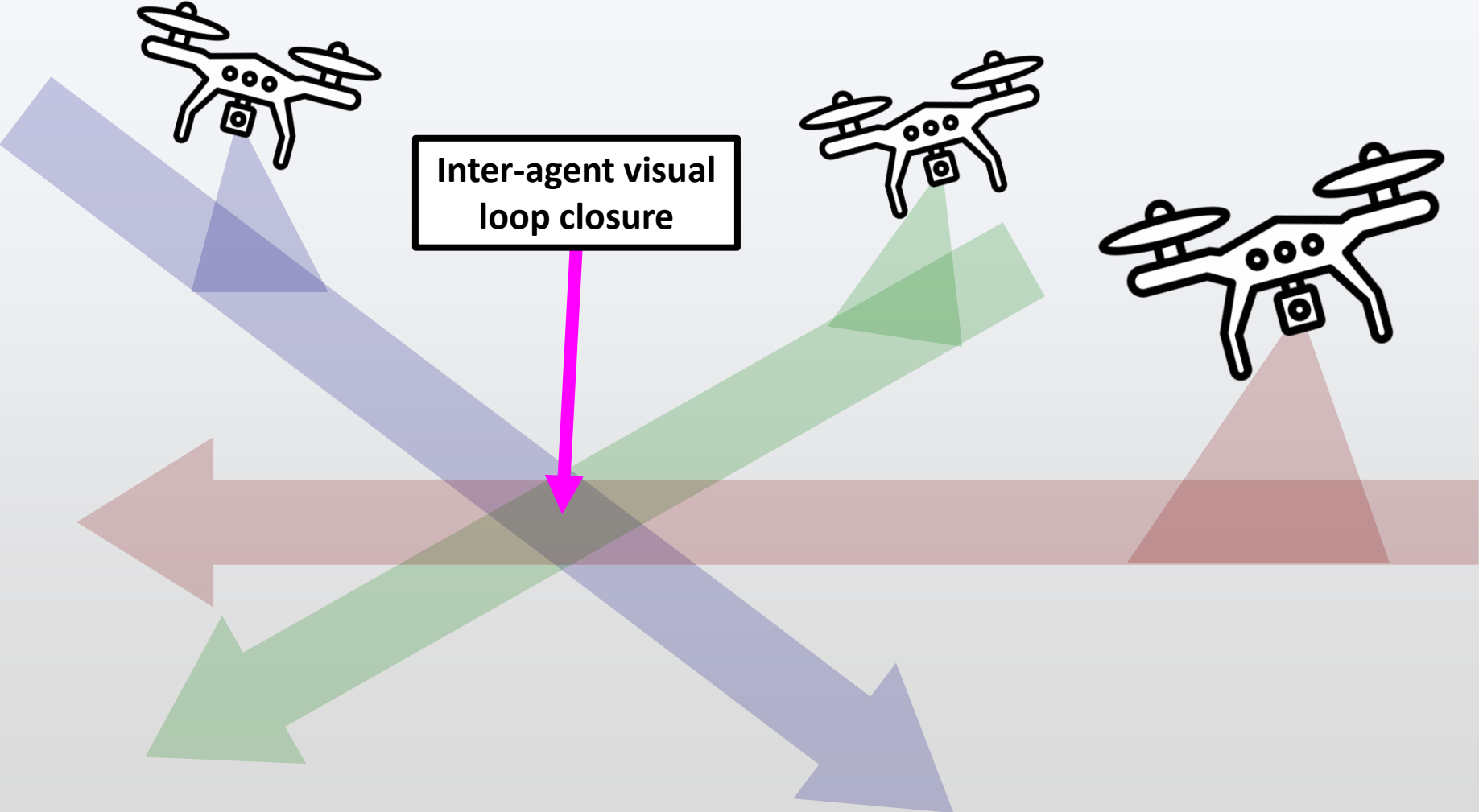
Motivation: Radiological Search

NG-LAMP on UAS



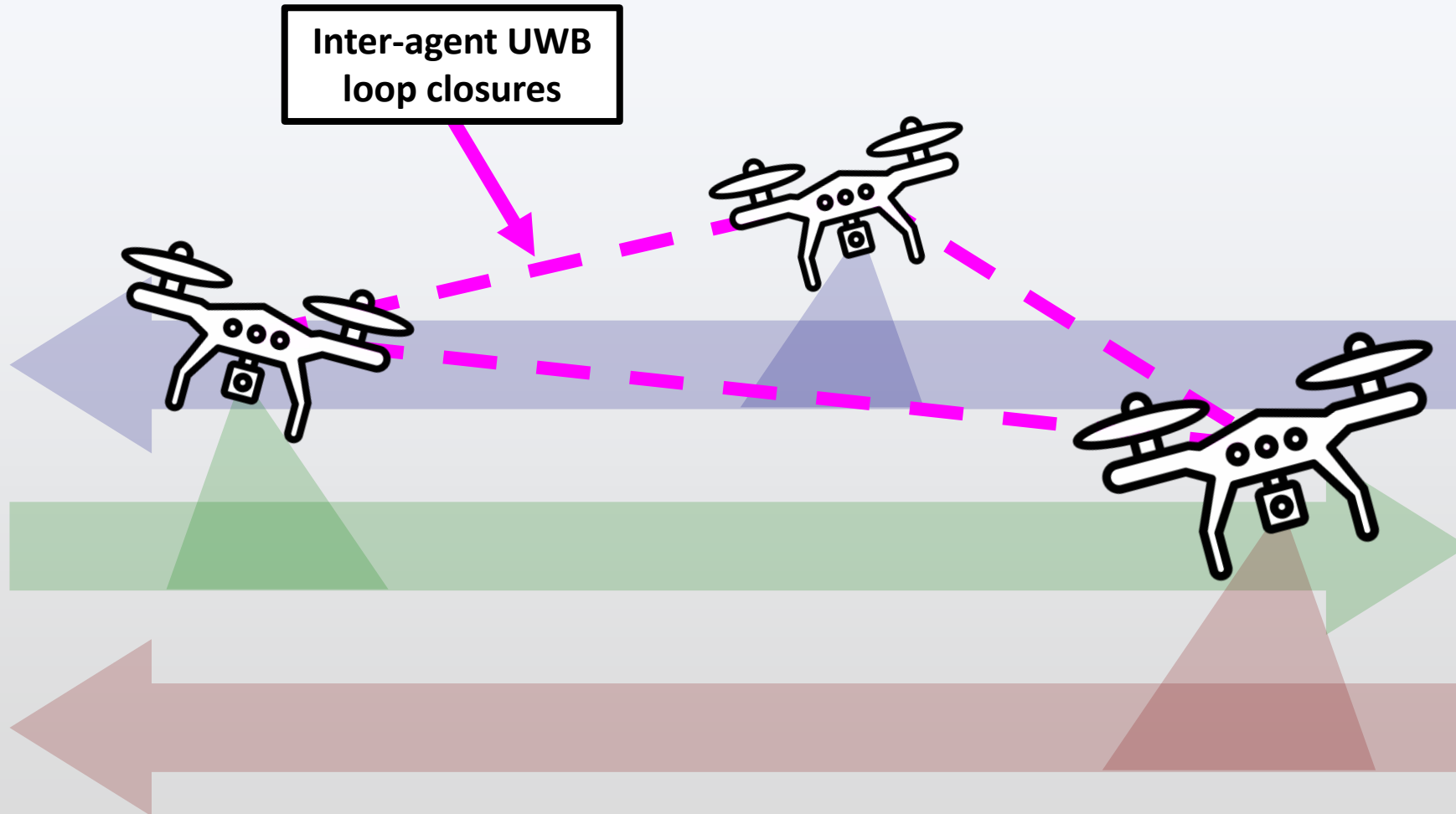
Goal: Leveraging prior work from our LBNL collaborators, we want to improve their state-of-the-art **LAMP detection system** by extending it to a multi-agent system.

Motivation: Multi-Agent Radiological Search



Typical SLAM sensors require agents to **cross paths** to **fuse their local maps**.

Motivation: Multi-Agent Radiological Search

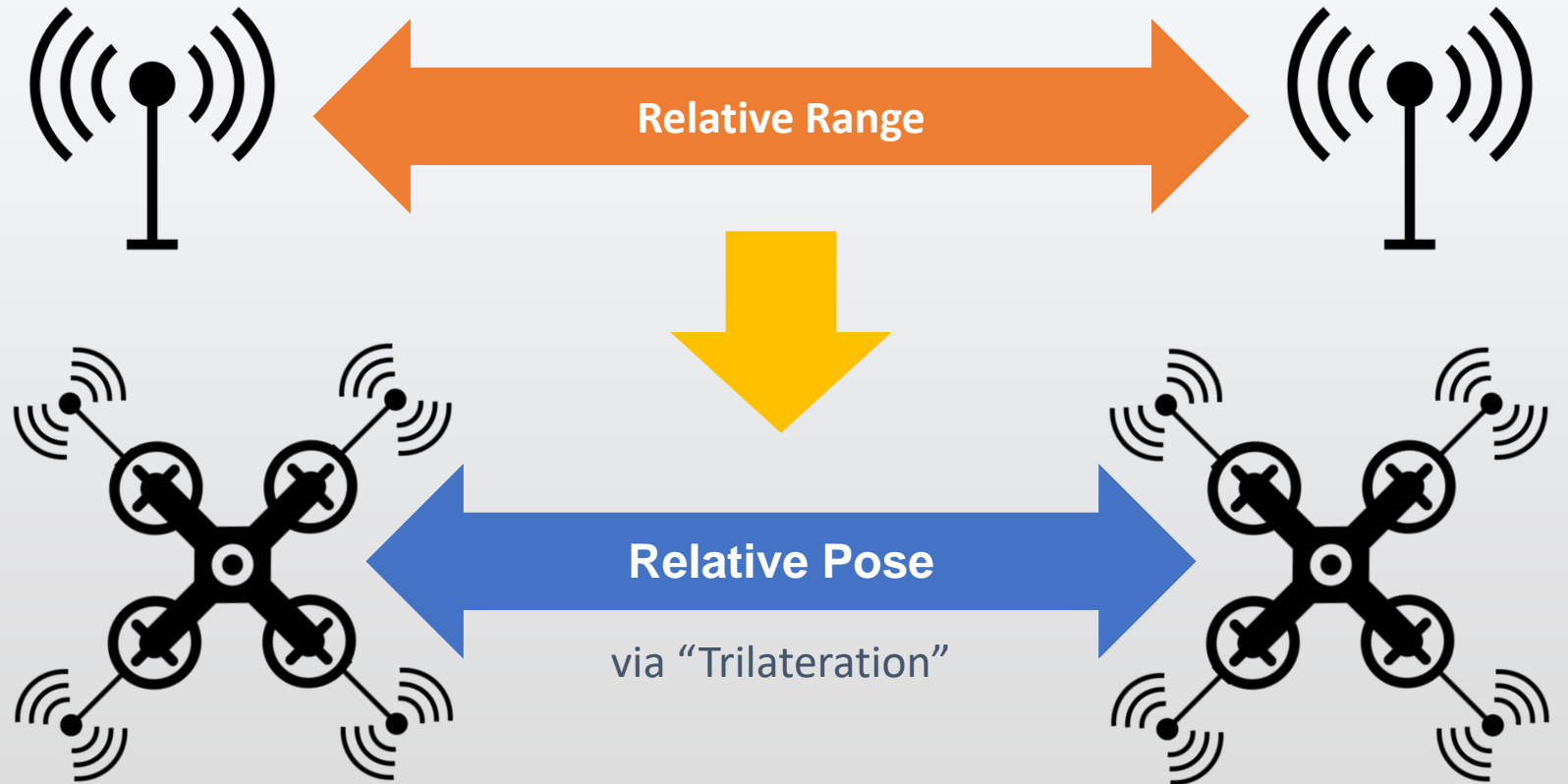


Using **ultra-wideband sensors**, we can get regular relative pose estimates between agents, allowing us to **fuse local maps without crossing paths**.

Ultra-Wideband Relative Pose Estimation

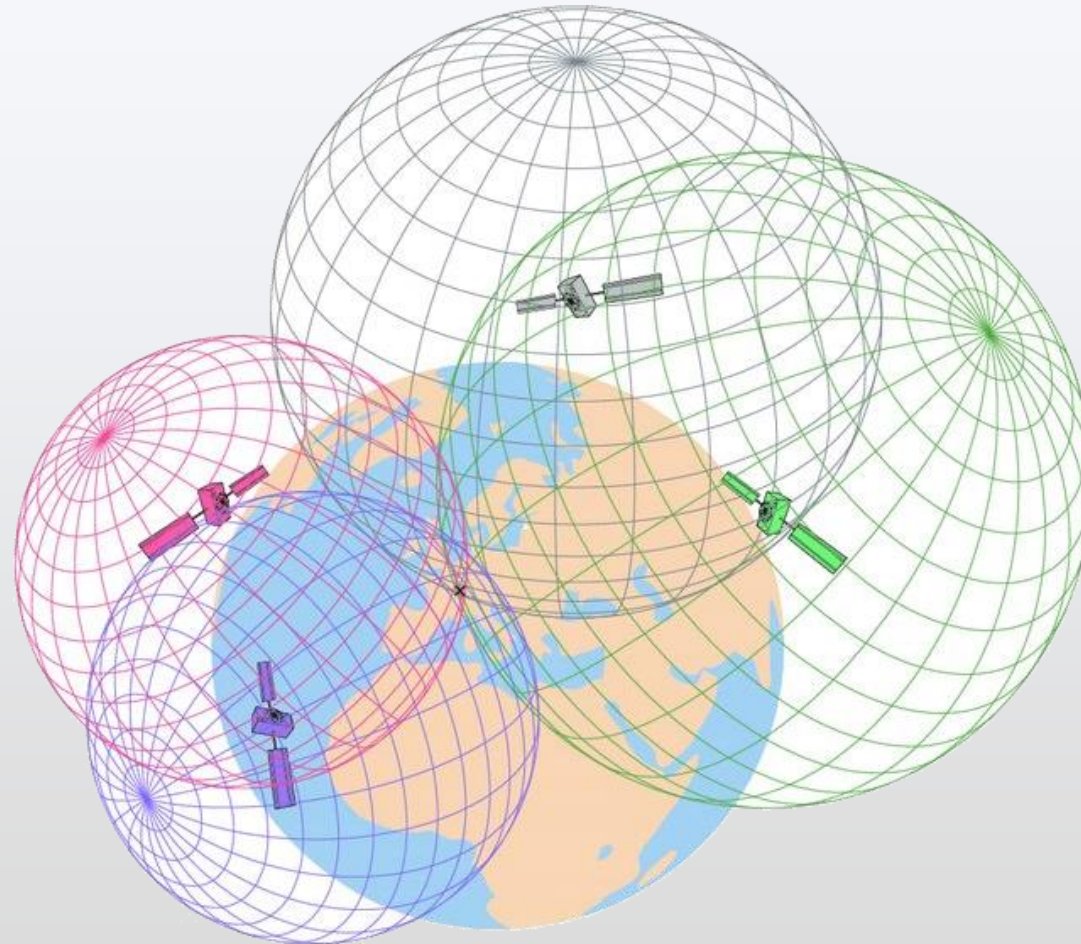


NoopLoop LinkTrack P-B



By placing multiple UWB sensors on each agent in a known configuration, we can use **instantaneously estimate relative pose.**

Ultra-Wideband Relative Pose Estimation



**This is conceptually similar to GPS multilateration.
GPS has inspired a lot of our system's error analysis techniques.**

OUR WORK

Our Proposed System



MURP: Multi-Agent Ultra-Wideband Relative Pose Estimation with Constrained Communications in 3D Environments

Andrew Fishberg Brian Quiter Jonathan P. How

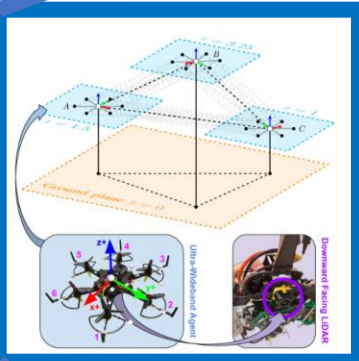
Abstract— Inter-agent relative localization is critical for many multi-robot systems operating in the absence of external positioning infrastructure or prior environmental knowledge. We propose a novel inter-agent relative 3D pose estimation system where each participating agent is equipped with several ultra-wideband (UWB) ranging tags. Prior work typically supplements noisy UWB range measurements with additional continuously transmitted data, such as odometry, leading to potential scaling issues with increased team size and/or decreased communication network capability. By equipping each agent with multiple UWB antennas, our approach addresses these concerns by using only locally collected UWB range measurements, a priori state constraints, and detections of when said constraints are violated. Leveraging our learned mean ranging bias correction, we gain a 19% positional error improvement giving us experimental mean absolute position and heading errors of 0.24m and 9.5° respectively. When compared to other state-of-the-art approaches, our work demonstrates improved performance over similar systems, while remaining competitive with methods that have significantly higher communication costs. Additionally, we make our datasets available.

I. INTRODUCTION

Multi-robot systems can be used to improve the efficiency and robustness of large-scale tasks such as search & rescue [1], warehouse automation [2], and planetary exploration [3]. To operate and parallelize effectively, these systems typically need to know where the agent (and its peers) are located in a common reference frame. In practice this is often achieved by localizing within an *a priori* map or using an external measurement system like GPS or motion capture (mocap) [4], [5]. If these technologies are unavailable or infeasible, common approaches utilize both relative localization [6] and multi-agent SLAM [7] techniques.

Within the last decade, ultra-wideband (UWB) has matured into a reliable, inexpensive, and commercially available RF solution for data transmission, relative ranging, and localization – UWB now comes as standard issue in many popular smartphone devices [8]. For robotics, UWB has several properties of note: precision of approximately 10cm, ranges up to 100m, resilience to multipath, operates in non-line of sight (NLOS) conditions, low power consumption, and 100Mbit/s communication speeds [9]. Recent devices even extend the recommended and operational ranges to 300m and 500m respectively [10]. Nevertheless, UWB measurements are not immune from ranging errors or noise (see Section III-A), the modeling and correction of which is an active area of research [11]–[14].

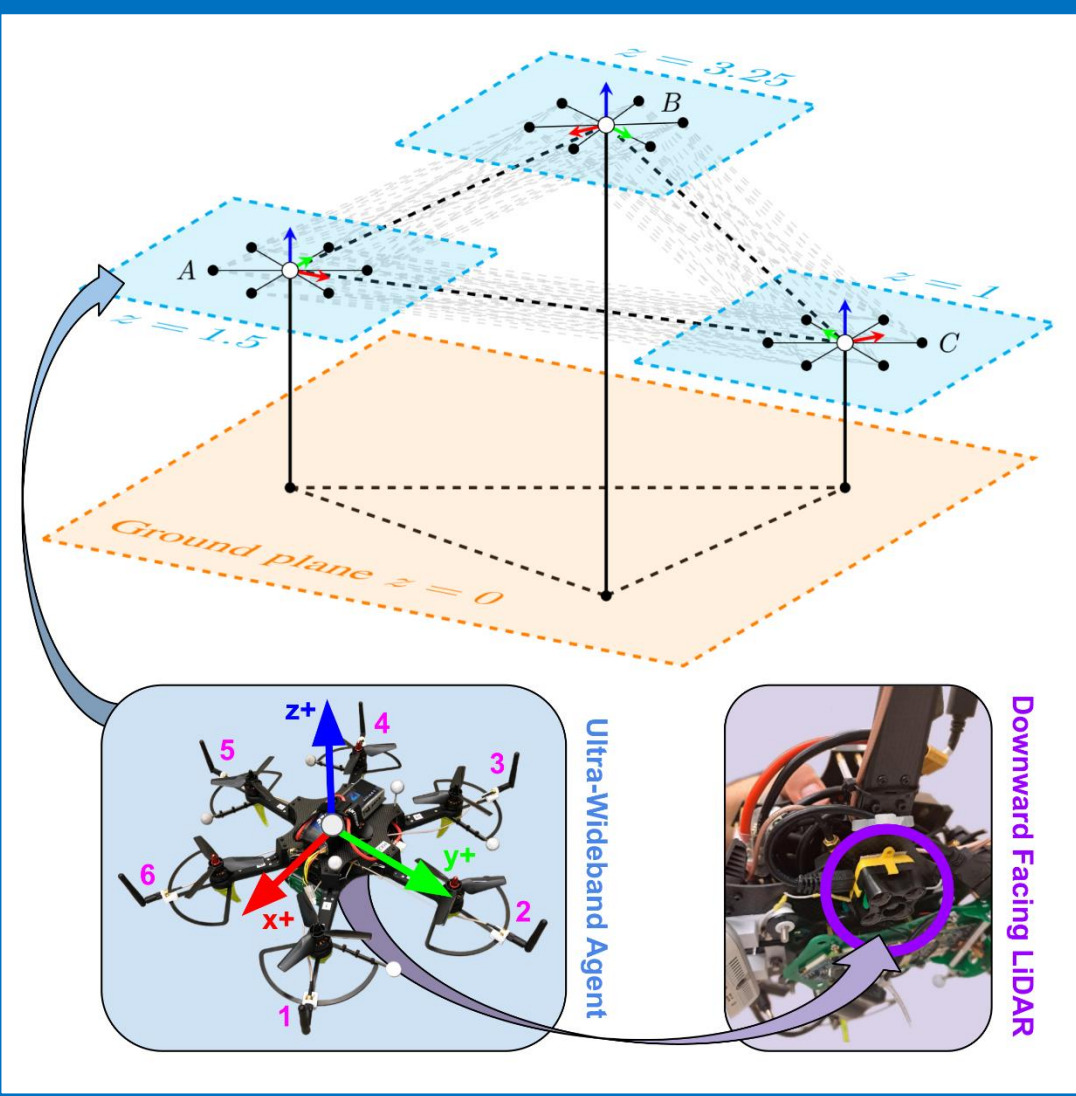
* Work supported in part by DOE, NNSA, and ALB funding. A. Fishberg and J. How are with MIT Department of Aeronautics and Astronautics, {fishberg, jhow}@mit.edu. B. Quiter is with Lawrence Berkeley National Laboratory, bquiter@lbl.gov.



... while performing real-time 3D relative pose estimation. Each agent is equipped with six ultra-wideband (UWB) antennas, each capable of performing pairwise relative ranging between all other agents' individual antennas. By using trilateration, an improved sensor model, and a priori state constraints about altitude/roll/pitch, agents can perform instantaneous estimation errors with locally collected UWB measurements (i.e., without the need to continuously transmit other measurements, such as odometry). Additionally, each agent locally monitors its a priori constraints via downward facing LiDAR and IMU, and thus only needs to transmit one-off messages with the swarm if these assumptions change or are violated.

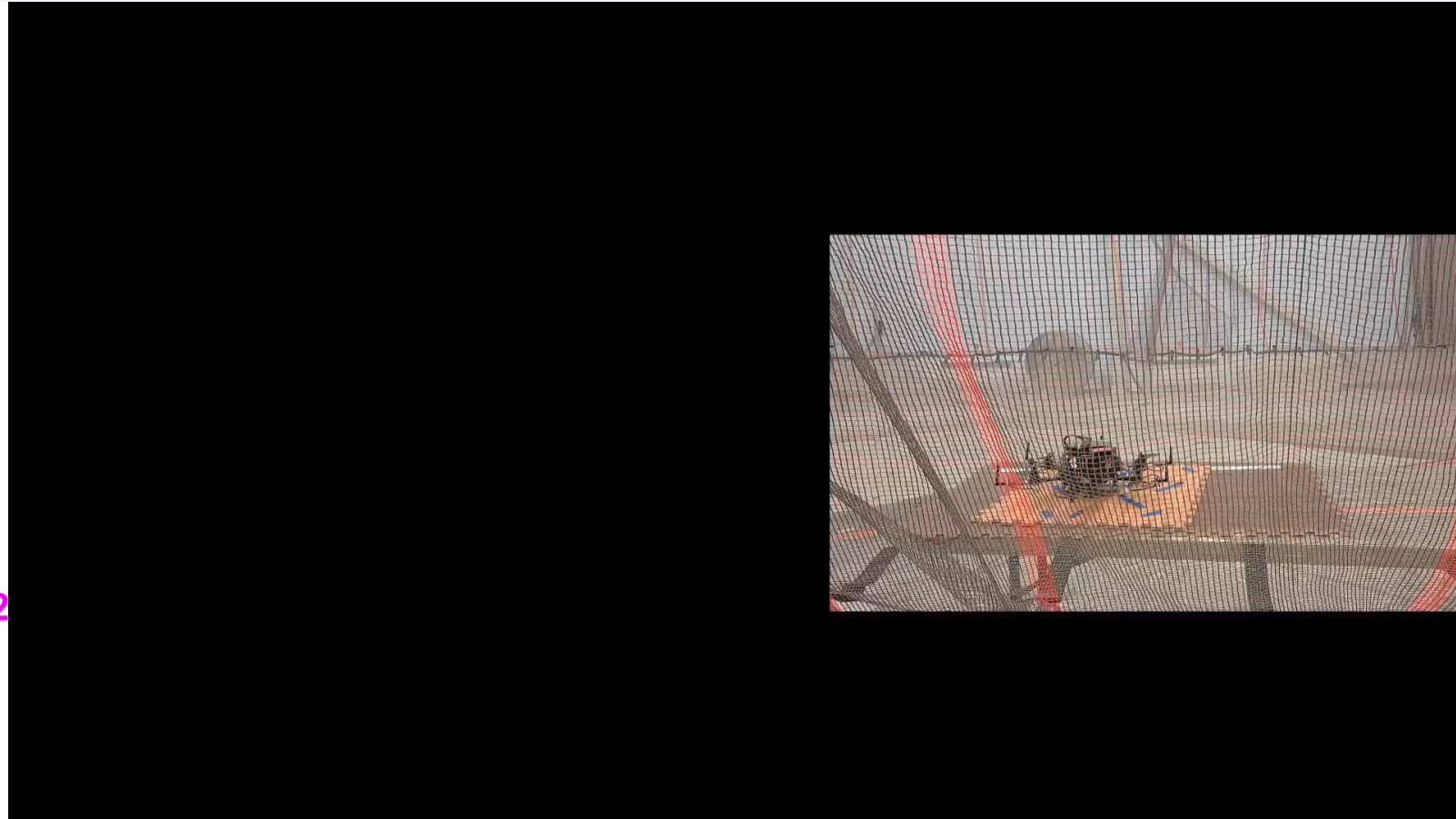
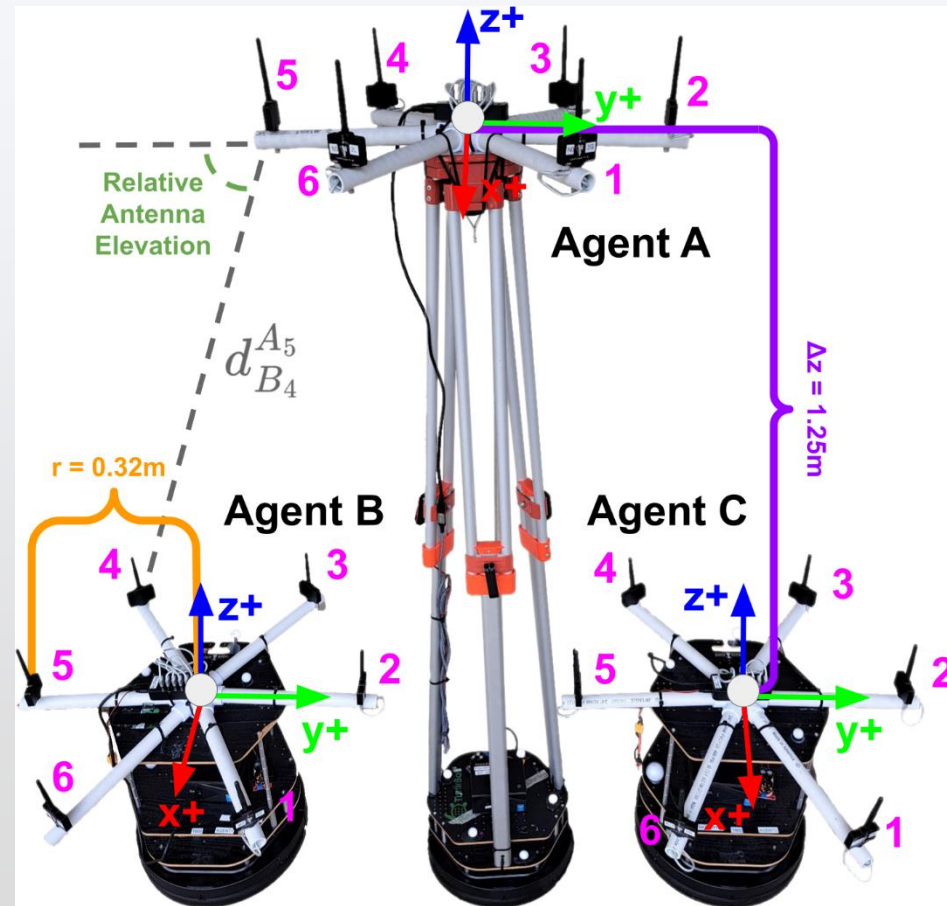
A common approach in UWB relative localization work fuses noisy UWB ranging measurements with additional continuously transmitted data, such as odometry [15] and visual inter-agent tracks [16], [17]. While these approaches achieve low absolute position error (APE) and also low heading error (AHE), there are two prevalent shortcomings. (1) They often use a simplistic UWB measurement noise model (e.g., zero mean Gaussian), which then requires the use of supplementary measurements to compensate. (2) Reliance on these supplementary measurements (often not locally collected, e.g. odometry), mandates their continuous transmission between agents, potentially impacting scalability to increased swarm size or decreased communication throughput.

Our previous work [18] used UWB to demonstrate an instantaneous multi-tag approach to relative 2D pose estimation that achieved superior mean position accuracy and competitive performance on other metrics to Cao et al. [15]



arXiv:2312.17731v1 [cs.RO] 29 Dec 2023

Data Collection

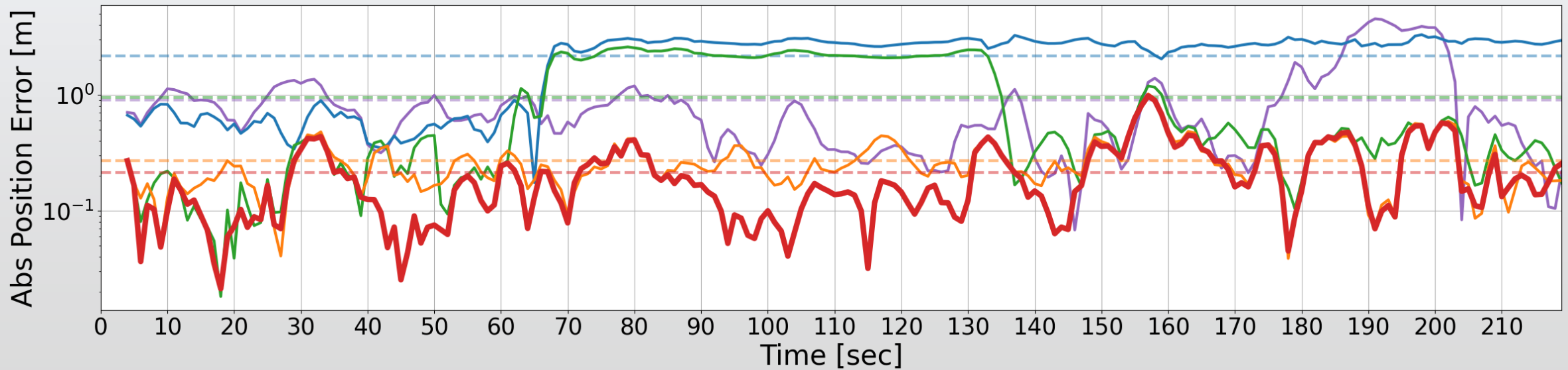


Collected nearly 6 hours of data, effectively creating **200+ hours** of pairwise measurements.

Our 3D Pose Results








Abs Position Error [m]				Scenarios (Section VI-B)														
				Trial 1			Trial 2			Trial 3			Trial 4			Trial 5		
color	el_bias	z_fixed	Huber	Mean	Max	Std	Mean	Max	Std	Mean	Max	Std	Mean	Max	Std	Mean	Max	Std
■	✓	✓	✓	2.21	4.40	1.17	0.89	4.50	0.88	2.37	4.82	1.13	2.26	4.58	1.12	2.77	4.32	0.59
				2.55	4.95	0.64	0.89	4.46	0.97	1.32	3.94	0.95	1.33	3.97	0.97	1.55	3.71	0.90
	✓	✓	✓	0.45	2.87	0.38	0.42	1.50	0.28	0.57	2.97	0.52	0.45	2.40	0.36	0.40	1.16	0.23
				0.34	2.86	0.43	0.34	1.49	0.32	0.53	2.96	0.55	0.38	2.41	0.39	0.30	1.16	0.28
■	✓		✓	1.14	3.29	1.12	2.15	3.29	1.03	1.24	3.60	1.01	2.30	3.57	1.02	1.30	3.24	1.16
■	✓		✓	0.44	1.64	0.30	0.95	2.58	0.90	0.85	3.10	0.75	0.85	2.69	0.82	1.44	2.88	0.90
■		✓	✓	0.29	0.91	0.14	0.27	1.02	0.14	0.32	1.03	0.20	0.28	0.78	0.14	0.29	0.71	0.13
■	✓	✓	✓	0.22	0.90	0.17	0.21	0.98	0.16	0.30	0.97	0.21	0.23	0.75	0.15	0.22	0.63	0.14



Experimental mean absolute position and heading errors of **0.24m and 9.5°** respectively across all experimental trials.

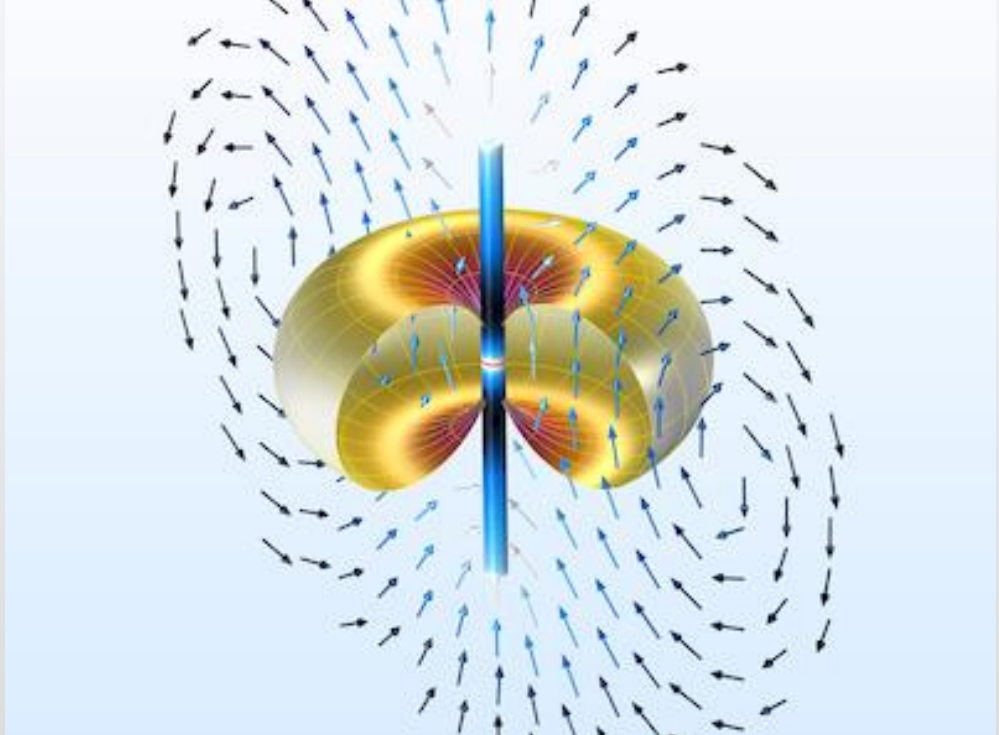
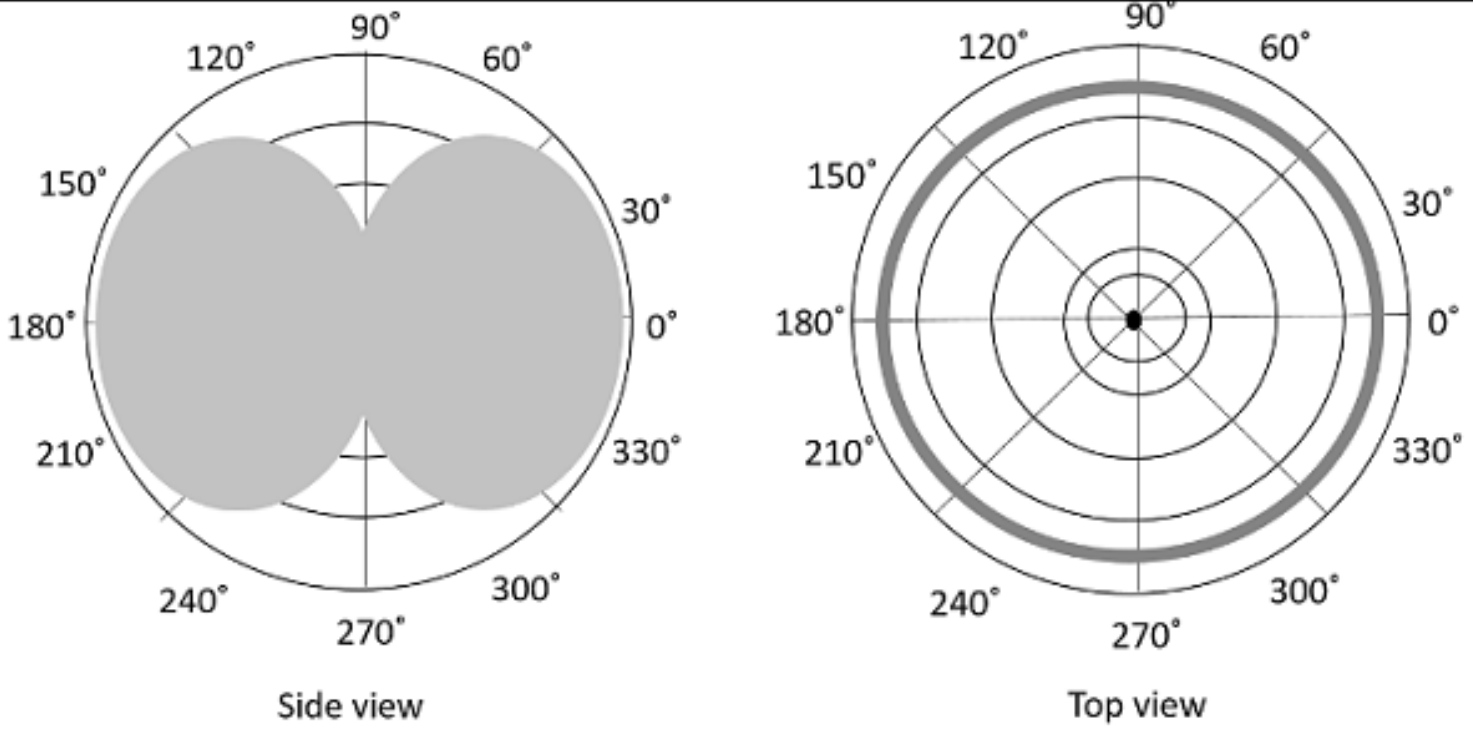
What is our “special sauce”?

Abs Position Error [m]			
color	el_bias	z_fixed	Huber
	✓	✓	
	✓	✓	
			✓
	✓		✓
		✓	✓
	✓	✓	✓

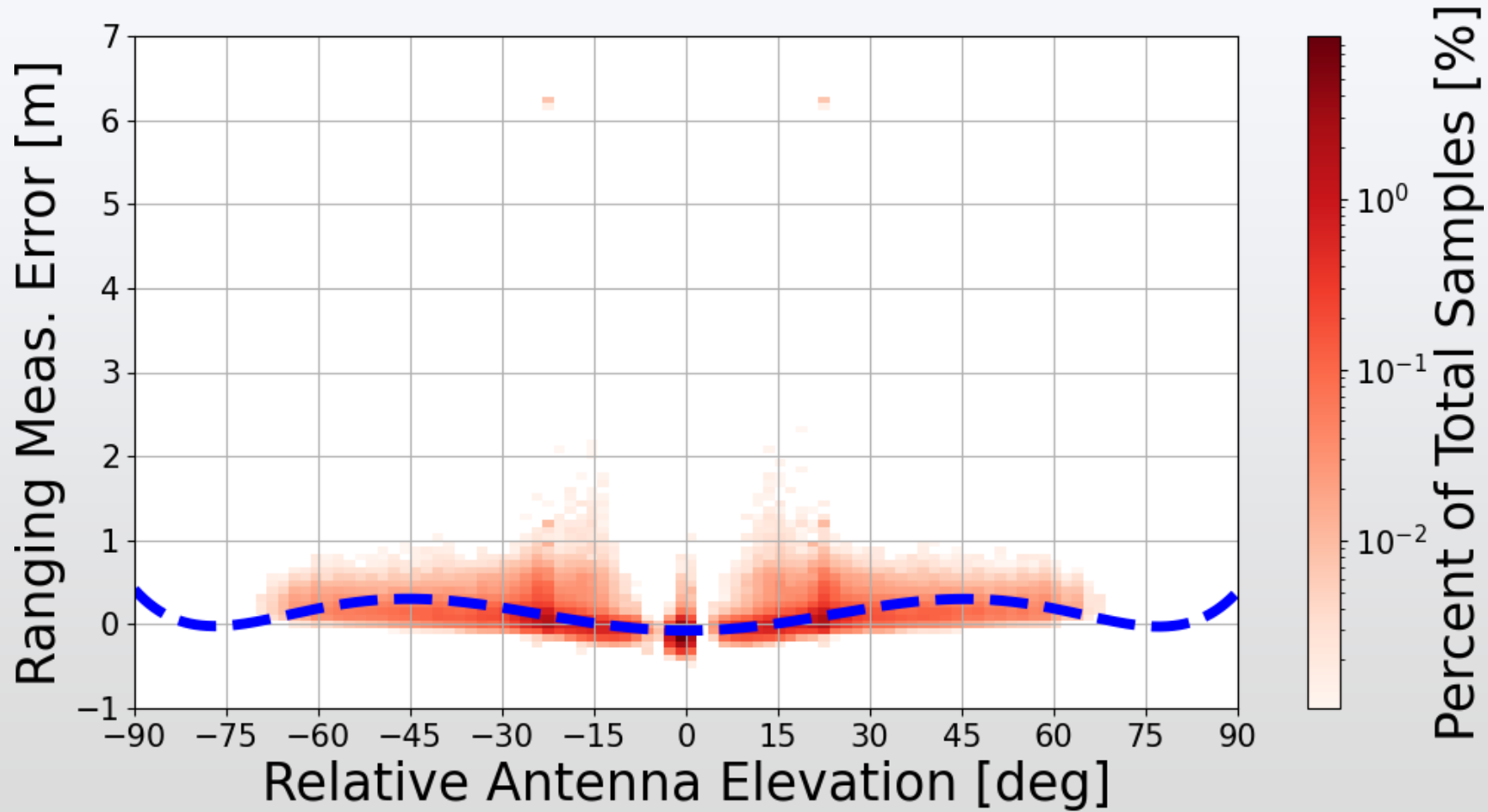
What is our “special sauce”?

Abs Position Error [m]			
color	el_bias	z_fixed	Huber
■	✓	✓	
	✓	✓	
■			✓
■	✓		✓
■		✓	✓
■	✓	✓	✓

Measurement Bias w.r.t. Relative Pose

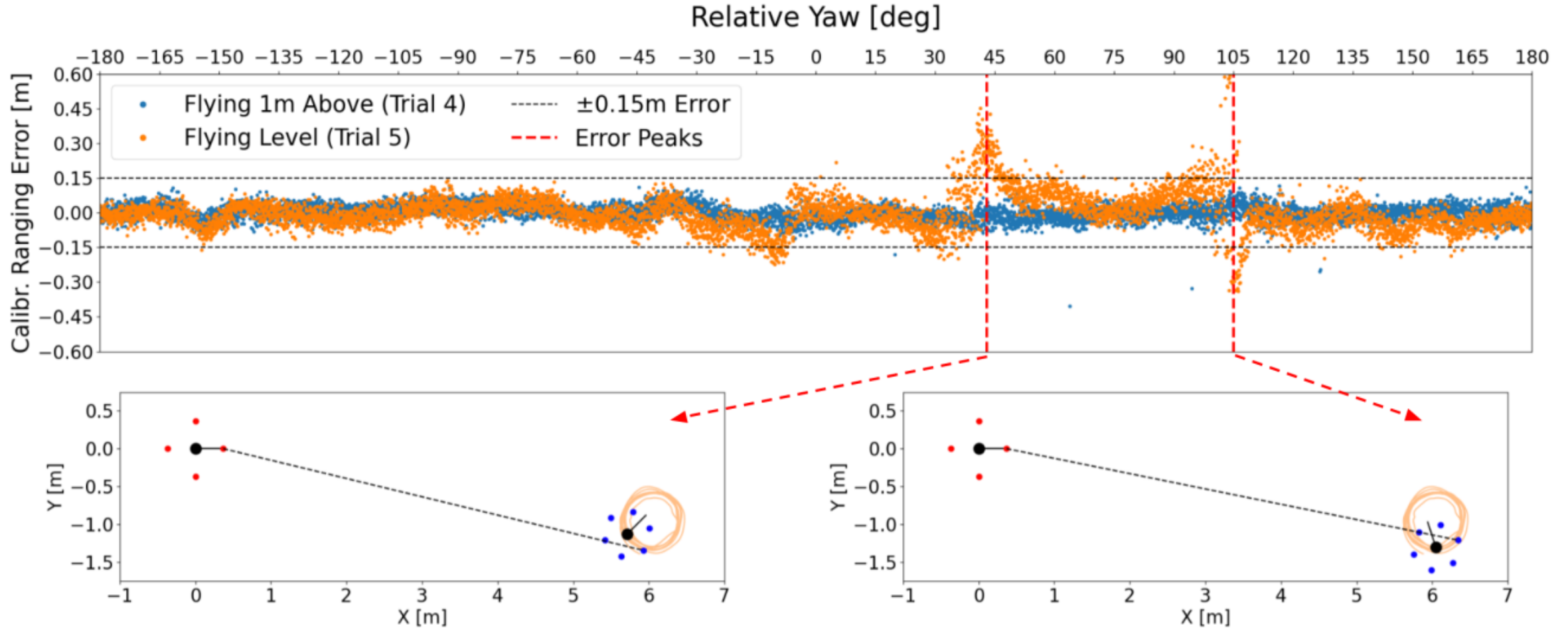


Measurement Bias w.r.t. Relative Pose



Measurement mean bias and variance **varies with relative elevation.**

Measurement Bias w.r.t. Relative Pose



Robot's body frame can cause **predictable measurement error.**

What is our “special sauce”?

Abs Position Error [m]			
color	el_bias	z_fixed	Huber
■	✓	✓	
	✓	✓	
■			✓
■	✓		✓
■		✓	✓
■	✓	✓	✓

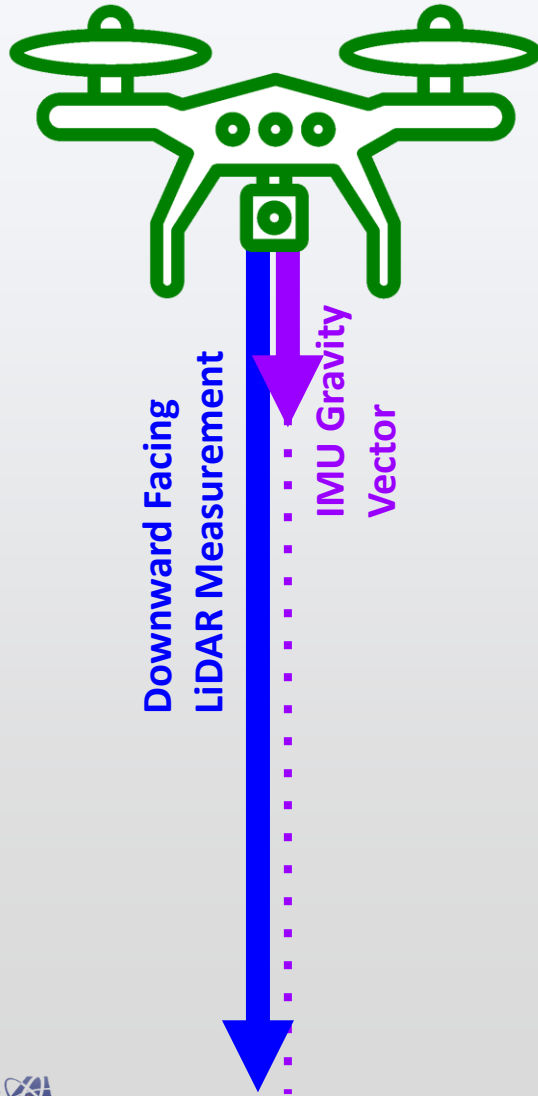
Assumptions that improve results



$$\min_{\mathbf{T}_B^A \in SE(3)} \sum_{i=1}^{N_A} \sum_{j=1}^{N_B} \ell \left(e_{B_j}^{A_i} (\mathbf{T}_B^A) \right)$$

$$e_{B_j}^{A_i} (\mathbf{T}_B^A) \triangleq \underbrace{\left(\tilde{d}_{B_j}^{A_i} - \bar{d}_{B_j}^{A_i} (\mathbf{T}_B^A) \right)}_{\text{bias adjusted measurement}} - \underbrace{d_{B_j}^{A_i} (\mathbf{T}_B^A)}_{\text{expected measurement}}$$

Assumptions that improve results



Reasonable assumptions for standard multi-rotors operation:

1. We can align the relative frames with respect to gravity.
2. We can *locally* measure our “global” roll/pitch w.r.t. gravity.
3. We can *locally* measure “global” altitude via barometer or downward facing LiDAR.
4. Non-stunt flight has relatively constrained roll/pitch (i.e., level flight) and maintains tight altitude envelop.

Assumptions that improve results



$$\min_{\mathbf{T}_B^A \in SE(3)} \sum_{i=1}^{N_A} \sum_{j=1}^{N_B} \ell \left(e_{B_j}^{A_i}(\mathbf{T}_B^A) \right)$$

$$e_{B_j}^{A_i}(\mathbf{T}_B^A) \triangleq \underbrace{\left(\tilde{d}_{B_j}^{A_i} - \bar{d}_{B_j}^{A_i}(\mathbf{T}_B^A) \right)}_{\text{bias adjusted measurement}} - \underbrace{d_{B_j}^{A_i}(\mathbf{T}_B^A)}_{\text{expected measurement}}$$

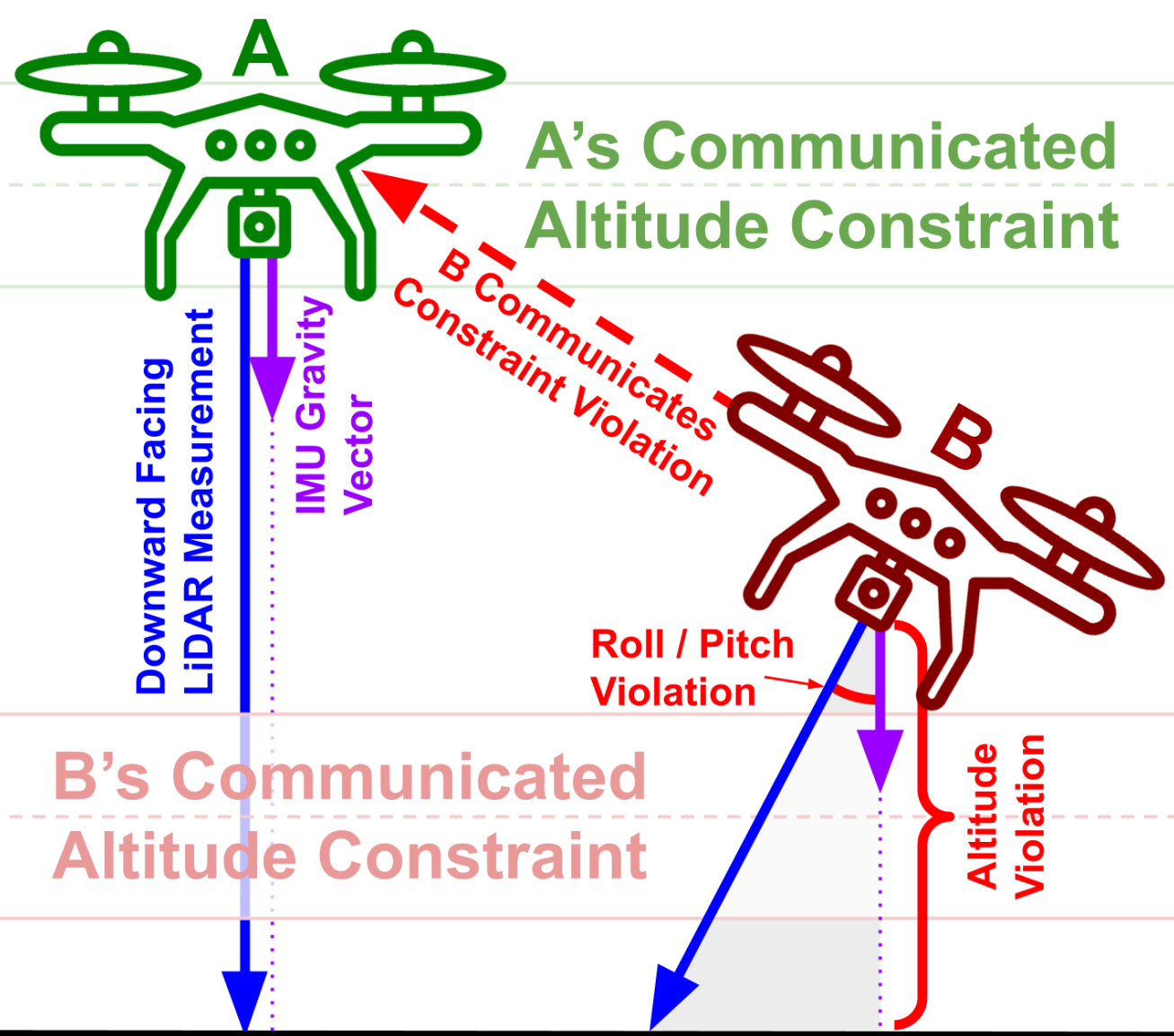
Assumptions that improve results



$$\min_{\substack{x_B^A, y_B^A \in \mathbb{R} \\ \gamma_B^A \in [-180^\circ, 180^\circ]}} \sum_{i=1}^{N_A} \sum_{j=1}^{N_B} \ell \left(e_{B_j}^{A_i} \left(\mathbf{T} \left(\underbrace{x_B^A, y_B^A}_{\text{free}}, \underbrace{\hat{z}_B^A, \hat{\alpha}_B^A, \hat{\beta}_B^A}_{\text{constrained}}, \underbrace{\gamma_B^A}_{\text{free}} \right) \right) \right)$$

$$e_{B_j}^{A_i} (\mathbf{T}_B^A) \triangleq \underbrace{\left(\tilde{d}_{B_j}^{A_i} - \bar{d}_{B_j}^{A_i} (\mathbf{T}_B^A) \right)}_{\text{bias adjusted measurement}} - \underbrace{d_{B_j}^{A_i} (\mathbf{T}_B^A)}_{\text{expected measurement}}$$

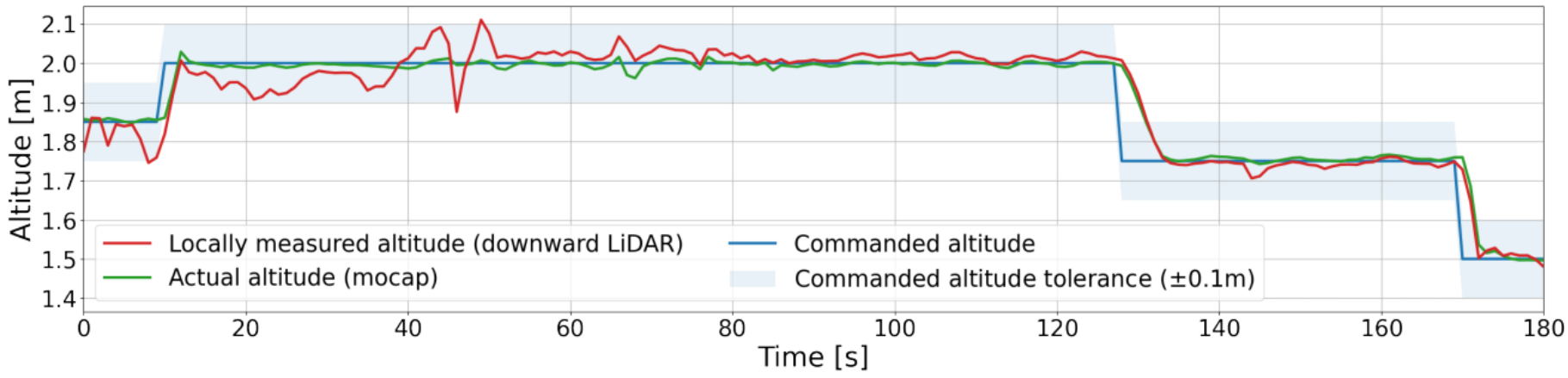
Assumptions that improve results



Assumptions that improve results



Abs Position Error [m]		Scenarios (Section VI-A)								
		Trial 1			Trial 2			Trial 3		
color	alt constraint	Mean	Max	Std	Mean	Max	Std	Mean	Max	Std
	z_free	1.17	2.83	1.06	1.04	1.53	0.24	0.45	0.94	0.19
■	z_comm	0.26	0.45	0.09	0.28	0.87	0.14	0.25	0.64	0.13
■	z_meas	0.26	0.44	0.09	0.27	0.87	0.14	0.24	0.66	0.14
■	z_true	0.25	0.44	0.10	0.26	0.87	0.15	0.22	0.64	0.14



Realistic sensor performance bounds makes it better to **assume z and monitor it** than leave it free.

What is our “special sauce”?

Abs Position Error [m]			
color	el_bias	z_fixed	Huber
■	✓	✓	
■	✓	✓	
■			✓
■	✓		✓
■		✓	✓
■	✓	✓	✓

HOW IS OUR WORK DIFFERENT?

Comparison to “Omni-Swarm”



3374

IEEE TRANSACTIONS ON ROBOTICS, VOL. 38, NO. 6, DECEMBER 2022

Omni-Swarm: A Decentralized Omnidirectional Visual–Inertial–UWB State Estimation System for Aerial Swarms

Hao Xu, Yichen Zhang, Boyu Zhou, Luqi Wang, Xinjie Yao, Guotao Meng, and Shaojie Shen

Abstract—Decentralized state estimation is one of the most fundamental components of autonomous aerial swarm systems in GPS-denied areas; yet, it remains a highly challenging research topic. Omni-swarm, a decentralized omnidirectional visual–inertial–ultrawideband (UWB) state estimation system for aerial swarms, is proposed in this article to address this research niche. To solve the issues of observability, complicated initialization, insufficient accuracy, and lack of global consistency, we introduce an omnidirectional perception front end in Omni-swarm. It consists of stereo wide-field-of-view cameras and UWB sensors, visual–inertial odometry, multi-drone map-based localization, and visual drone tracking algorithms. The measurements from the front end are fused with graph-based optimization in the back end. The proposed method achieves centimeter-level relative state estimation accuracy while guaranteeing global consistency in the aerial swarm, as evidenced by the experimental results. Moreover, supported by Omni-swarm, interdrone collision avoidance can be accomplished without any external devices, demonstrating the potential of Omni-swarm as the foundation of autonomous aerial swarms.

Index Terms—Aerial systems, multirobot systems, perception and autonomy, sensor fusion, swarms.

NOMENCLATURE

\hat{x}_i	Estimated state.
$d_{i,j}^t$	Distance between drone i and drone j at time t .
\mathcal{F}_k^t	Keyframe of the drone k at time t , which contains the 4-D pose ${}^{i_a}P_{k^t}$ to be estimated, a few virtual camera keyframes $\mathcal{K}_{k^t}^c$, and other essential information of the drone.
$\mathcal{K}_{k^t}^c$	Keyframe of drone k 's virtual camera c at time t , which contains the global descriptor, local features,

\mathcal{SF}_k^t	Swarm keyframe of the drone k at time t , which contains n keyframes.
G_k	Graph built on drone k for state estimation.
$(\cdot)_R$	Rotation part of the transformation matrix.
$(\cdot)_T$	Translation part of the transformation matrix.
$(\cdot)_x$	Corresponding four-DoF transformation matrix.
$(\cdot)_y$	Corresponding six-DoF transformation matrix.
$(\cdot)_z$	Translation part of the transformation matrix.
$(\cdot)_\omega$	Measurement data at time t .
$(\cdot)_\psi$	Yaw angle of the rotation matrix.
$(\mathcal{F})_f$	Global descriptor of the keyframe \mathcal{F} .
$(\mathcal{K})_c$	Corresponding keyframe \mathcal{F}_k^t of virtual camera keyframe \mathcal{K} .

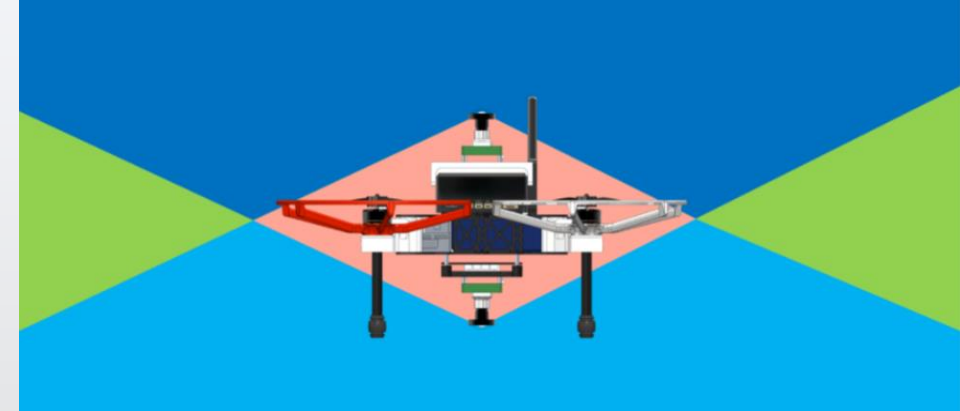
$(\mathcal{F})_f$	Local descriptors of the features of the keyframe \mathcal{F} .
$\ (\cdot)\ $	Euclidean norm of (\cdot) if (\cdot) is a vector or matrix; otherwise, $\ (\cdot)\ $ is its size.
$\ (\cdot)\ _\Sigma$	Mahalanobis norm of (\cdot) .
\mathcal{D}	Set of all the existing drones, including the currently unavailable drones due to loss of communication, user poweroff, and accident.

\mathcal{D}_k^a	Set of all available drones for drone k .
\mathcal{D}_k^e	Set of all estimated drones of drone k 's state estimation.
\mathcal{D}_k^u	Set of all uninitialized drones of drone k 's state estimation, where $\mathcal{D}_k^u = \mathcal{D}_k^a - \mathcal{D}_k^e$.
$b_i^j(\cdot)_i^j$	State of drone i in drone k 's body frame. For simplicity, the pose in the body frame is defined as a four-DoF pose, i.e., $b_i^j(\cdot)_i^j = ({}^{i_a}P_{k^t})^{-1}v_i(\cdot)_i$, i th drone.
D_i	State of drone i in drone i 's local frame.

${}^{i_a}(\cdot)_i^j$	Equal to $\begin{bmatrix} R_i & ({}^{i_a}v)_i^j & {}^{i_a}X_{i^t} \\ 0 & 0 & 1 \end{bmatrix}$. The pose of drone i in drone k 's local frame at time t . For simplicity, the notation of P_{i^t} represents ${}^{i_a}P_{i^t}$. ${}^{i_a}R_i$ (${}^{i_a}\psi_i^j$) represents the rotation matrix rotated over the z -axis with angle ${}^{i_a}\psi_i^j = ({}^{i_a}R_i)_\omega$.
${}^{i_a}P_{i^t}$	Equal to $\begin{bmatrix} {}^{i_a}R_i & {}^{i_a}X_{i^t} \\ 0 & 1 \end{bmatrix}$. The six-DoF pose of drone i in drone k 's local frame at time t . ${}^{i_a}R_i$ represents the rotation matrix.

${}^{i_a}T_{i^t}$	Four- and six-DoF pose, respectively, of drone k in its local frame, as estimated by VIO, which drifts
$\hat{P}_{k^t}, \hat{T}_{k^t}$	

virtual camera's extrinsic, and other essential information of the drone. The virtual camera c is cropped from the raw fisheye camera.
Equal to $\{\mathcal{F}_k^t, \mathcal{F}_{k^t}^1, \dots, \mathcal{F}_{k^t}^n\}$. The swarm keyframe of the drone k at time t , which contains n keyframes.
Graph built on drone k for state estimation.
Rotation part of the transformation matrix.
Corresponding four-DoF transformation matrix.
Corresponding six-DoF transformation matrix.
Translation part of the transformation matrix.
Measurement data at time t .
Yaw angle of the rotation matrix.
Global descriptor of the keyframe \mathcal{F} .
Corresponding keyframe \mathcal{F}_k^t of virtual camera keyframe \mathcal{K} .
Local descriptors of the features of the keyframe \mathcal{F} .
Euclidean norm of (\cdot) if (\cdot) is a vector or matrix; otherwise, $\|(\cdot)\|$ is its size.
Mahalanobis norm of (\cdot) .
Set of all the existing drones, including the currently unavailable drones due to loss of communication, user poweroff, and accident.
Set of all available drones for drone k .
Set of all estimated drones of drone k 's state estimation.
Set of all uninitialized drones of drone k 's state estimation, where $\mathcal{D}_k^u = \mathcal{D}_k^a - \mathcal{D}_k^e$.
State of drone i in drone k 's body frame. For simplicity, the pose in the body frame is defined as a four-DoF pose, i.e., $b_i^j(\cdot)_i^j = ({}^{i_a}P_{k^t})^{-1}v_i(\cdot)_i$, i th drone.
State of drone i in drone i 's local frame.
Equal to $\begin{bmatrix} R_i & ({}^{i_a}v)_i^j & {}^{i_a}X_{i^t} \\ 0 & 0 & 1 \end{bmatrix}$. The pose of drone i in drone k 's local frame at time t . For simplicity, the notation of P_{i^t} represents ${}^{i_a}P_{i^t}$. ${}^{i_a}R_i$ (${}^{i_a}\psi_i^j$) represents the rotation matrix rotated over the z -axis with angle ${}^{i_a}\psi_i^j = ({}^{i_a}R_i)_\omega$.
Equal to $\begin{bmatrix} {}^{i_a}R_i & {}^{i_a}X_{i^t} \\ 0 & 1 \end{bmatrix}$. The six-DoF pose of drone i in drone k 's local frame at time t . ${}^{i_a}R_i$ represents the rotation matrix.
Four- and six-DoF pose, respectively, of drone k in its local frame, as estimated by VIO, which drifts



Manuscript received 12 December 2021; revised 25 March 2022; accepted 9 May 2022. Date of publication 1 July 2022; date of current version 6 December 2022. This work was supported in part by the Hong Kong University of Science and Technology (HKUST) Postgraduate Studentship, in part by the University Grants Committee of Hong Kong under Grant MGS20EG20, and in part by the HKUST-DJI Joint Innovation Laboratory. This paper was recommended for publication by Associate Editor L. Carlone and Editor P. Robuffo Giordano upon evaluation of the reviewers' comments. *Corresponding author: Hao Xu.*

The authors are with the Department of Electronic and Computer Engineering, Hong Kong University of Science and Technology, Hong Kong (e-mail: hxu@connect.ust.hk; yzhangce@connect.ust.hk; bzhouai@connect.ust.hk; lqwang@connect.ust.hk; yzhaoyb@connect.ust.hk; gmeng@connect.ust.hk; eshaojie@ust.hk).

This article has supplementary material provided by the authors and color versions of one or more figures available at <https://doi.org/10.1109/TRO.2022.3182503>.

Digital Object Identifier 10.1109/TRO.2022.3182503

1552-3098 © 2022 IEEE. Personal use is permitted, but republication/redistribution requires IEEE permission. See https://www.ieee.org/publications_standards/publications/rights/index.html for more information.

Authorized licensed use limited to: MIT Libraries. Downloaded on February 16, 2024 at 16:40:19 UTC from IEEE Xplore. Restrictions apply.

Omni-Swarm uses a single UWB antenna, **omni-direction camera**, and SLAM techniques to perform swarm localization.

Comparison to “Omni-Swarm”



$$\begin{aligned} \min_{\mathcal{X}_k} & \left\{ \sum_{(i,t) \in \mathcal{S}} \left\| \mathbf{r}_{\mathcal{RP}} \left(\mathbf{z}_{\delta \mathbf{P}_i}^t, \mathcal{X}_k \right) \right\|_{\Sigma}^2 \right. && \longleftarrow \text{Odometry factors} \\ & + \sum_{(i,j,t) \in \mathcal{U}} \rho \left(\left\| \mathbf{r}_d \left(\mathbf{z}_{d_{ij}}^t, \mathcal{X}_k \right) \right\|_{\Sigma}^2 \right) && \longleftarrow \text{Distance factors} \\ & + \sum_{(i,j,t) \in \mathcal{VD}} \rho \left(\left\| \mathbf{r}_{\mathcal{RP}} \left(\mathbf{z}_{D_{i \rightarrow j}}^t, \mathcal{X}_k \right) \right\|_{\Sigma}^2 \right) && \longleftarrow \text{Visual factors} \\ & + \left. \sum_{\mathcal{L}_{k \rightarrow j}^{t_0 \rightarrow t_1} \in \mathcal{L}} \rho \left(\left\| \mathbf{r}_{\mathcal{RP}} \left(\mathbf{z}_{\mathcal{L}_{i \rightarrow j}}^{t_0 \rightarrow t_1}, \mathcal{X}_k \right) \right\|_{\Sigma}^2 \right) \right\} && \longleftarrow \text{Map-based factors} \end{aligned}$$

Omni-Swarm has a **similar optimization formulation**, but leverages a lot of **data transmitted from other agents**.

Comparison to “Omni-Swarm”



TABLE VI
COMPARISON OF SWARM STATE ESTIMATION METHODS ON THE INDOOR DATASETS

Dataset	Metrics	<i>Xu2020</i>		<i>PGO</i>		<i>VIO-only</i>		Proposed		<i>Without UWB</i>		<i>Without Tracking</i>		<i>Without Map-based</i>		<i>Without Outlier Rej.</i>	
		Pos	Rot	Pos	Rot	Pos	Rot	Pos	Rot	Pos	Rot	Pos	Rot	Pos	Rot	Pos	Rot
Parallel1	ATE	0.600	8.6°	0.149	2.5°	0.228	2.5°	0.127	2.2°	0.126	2.2°	0.149	2.3°	0.160	2.4°	0.360	2.6°
	RE	0.959	17.7°	0.114	3.3°	0.261	2.3°	0.062	2.3°	0.063	2.7°	0.100	3.7°	0.062	2.6°	0.064	2.3°
Parallel2	ATE	0.351	3.2°	0.113	3.2°	0.225	3.0°	0.086	3.0°	0.094	3.1°	0.096	4.3°	0.225	3.1°	0.119	3.2°
	RE	0.241	4.7°	0.124	4.3°	0.230	4.3°	0.063	4.3°	0.083	4.0°	0.096	4.3°	0.069	4.2°	0.069	4.3°
Parallel3	ATE	0.470	2.6°	0.153	1.8°	0.281	3.1°	0.119	1.8°	0.128	1.8°	0.134	1.7°	0.242	3.0°	0.535	5.1°
	RE	0.566	1.8°	0.130	1.7°	0.225	4.7°	0.072	1.8°	0.082	1.8°	0.081	1.8°	0.075	1.9°	0.143	4.0°
RandFlight	ATE	0.197	2.7°	0.153	1.8°	0.125	2.6°	0.088	2.7°	0.092	2.7°	0.101	2.7°	0.079	2.7°	0.165	5.9°
	RE	0.191	2.1°	0.130	1.7°	0.160	1.1°	0.069	1.3°	0.071	1.2°	0.078	1.4°	0.074	1.4°	0.147	9.8°

Init. Time. is the average time for successful initialization of state estimation. The overall best results in ATE and RE are in bold.

Proposed		<i>Without UWB</i>	
Pos	Rot	Pos	Rot
0.127	2.2°	0.126	2.2°
0.062	2.3°	0.063	2.7°
0.086	3.0°	0.094	3.1°
0.063	4.3°	0.083	4.0°
0.119	1.8°	0.128	1.8°
0.072	1.8°	0.082	1.8°
0.088	2.7°	0.092	2.7°
0.069	1.3°	0.071	1.2°

Visual tracks are doing most of Omni-Swarm’s “heavy lifting”, **not UWB.**

Advantages of Our Approach



Most papers in this space are not concerned with comms usage.

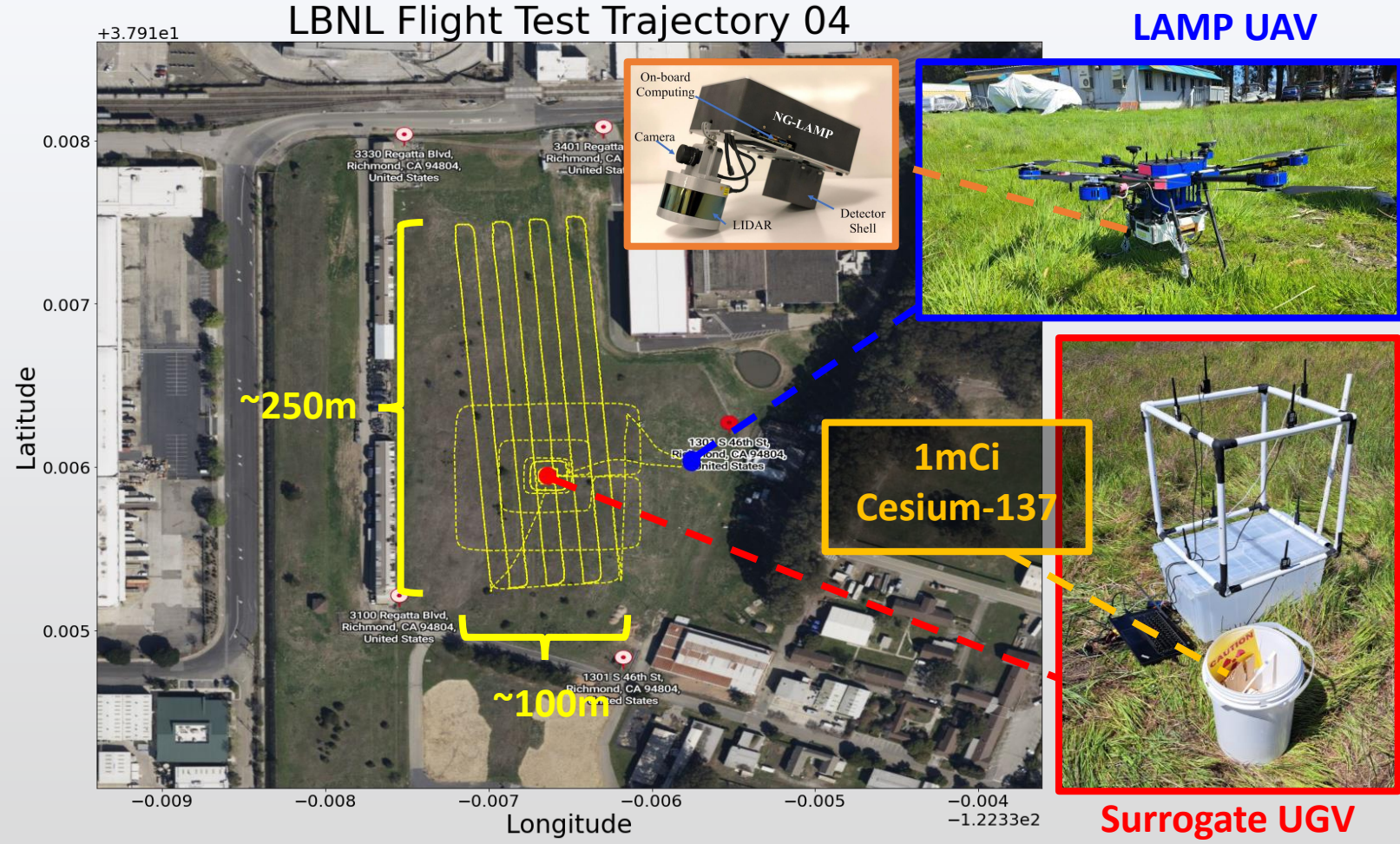
There are compelling reasons to worry about comms usage:

1. Large swarm, data transmission is $O(n^2)$
2. Limited comms budget can be better used elsewhere (e.g., visual loop closures, planning, etc.)
3. Data comms can be more finicky than a TOF measurement

We care about comms usage -- and we still achieve mean abs position and heading errors of **0.24m and 9.5°** respectively.

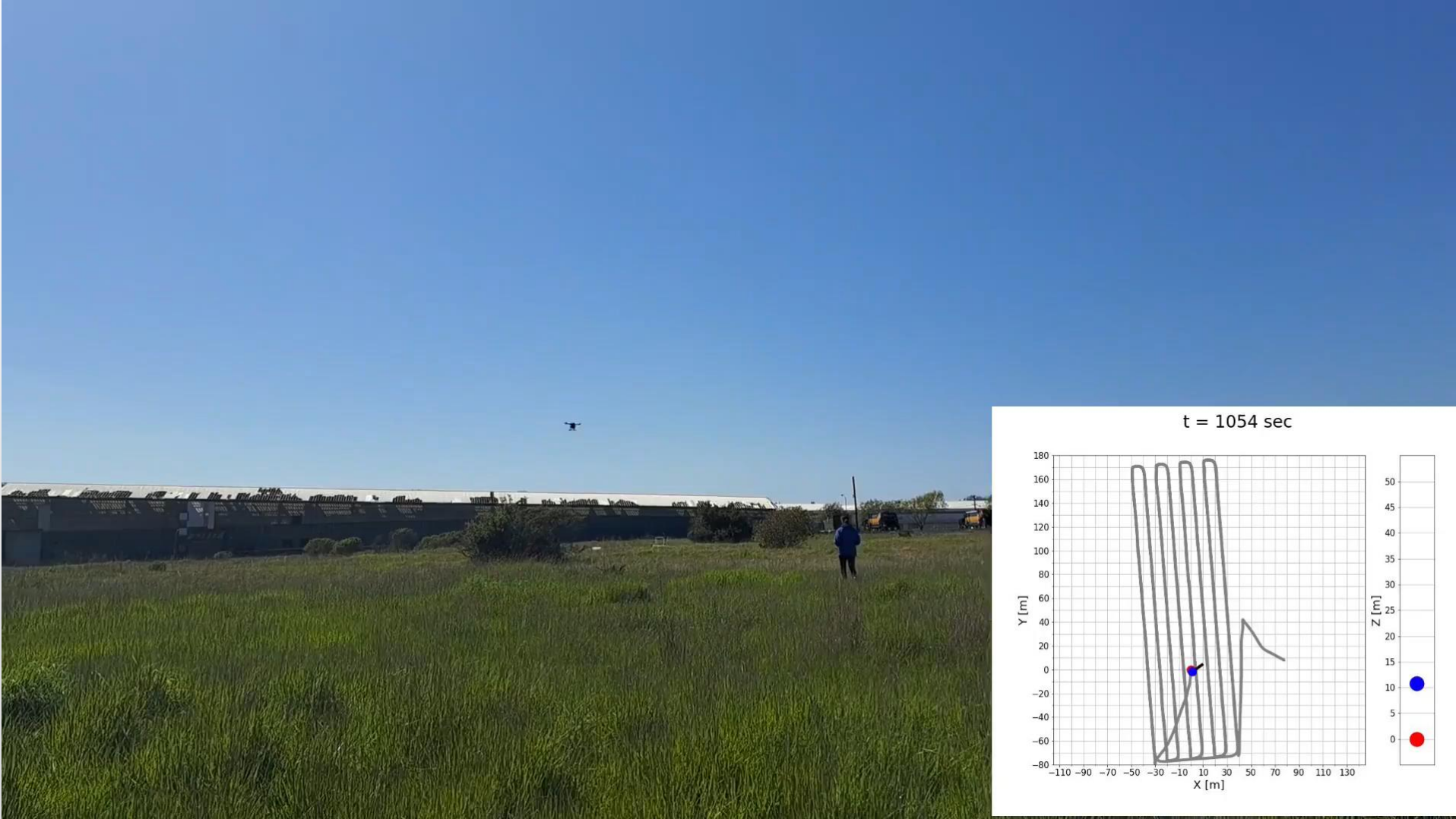
FUTURE WORK

Incorporating our error model into SLAM

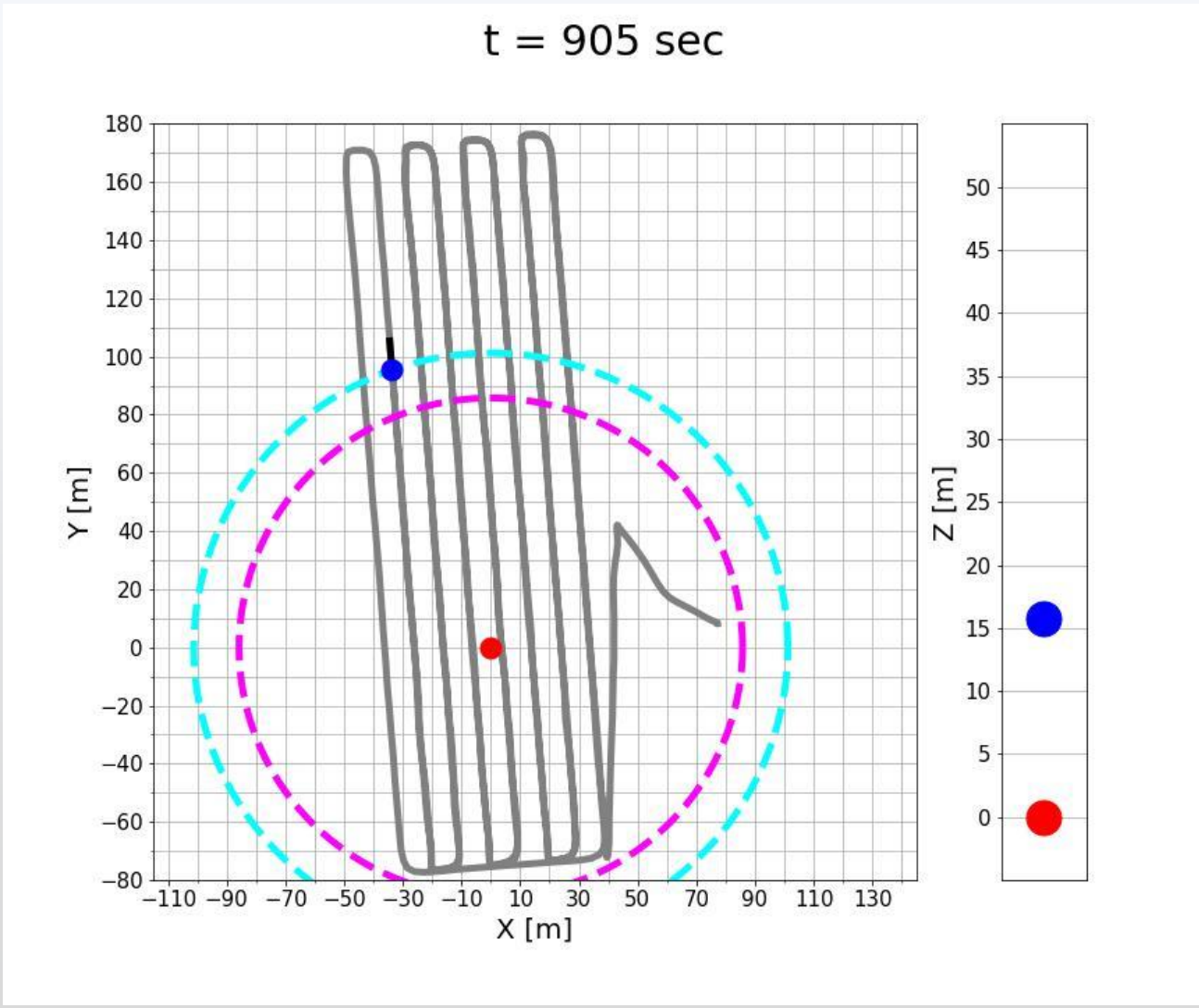


During our recent April LBNL flight tests, we collected over 2hrs worth of LAMP + UWB flight data with 1mCi of Cesium-137 in the field.

Incorporating our error model into SLAM



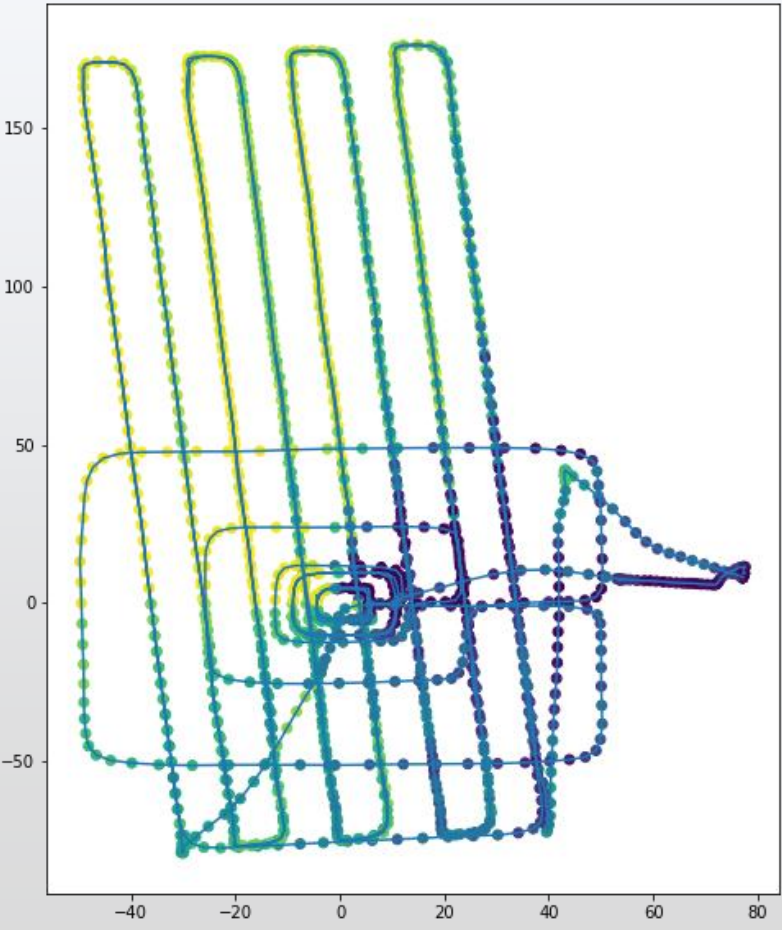
Incorporating our error model into SLAM



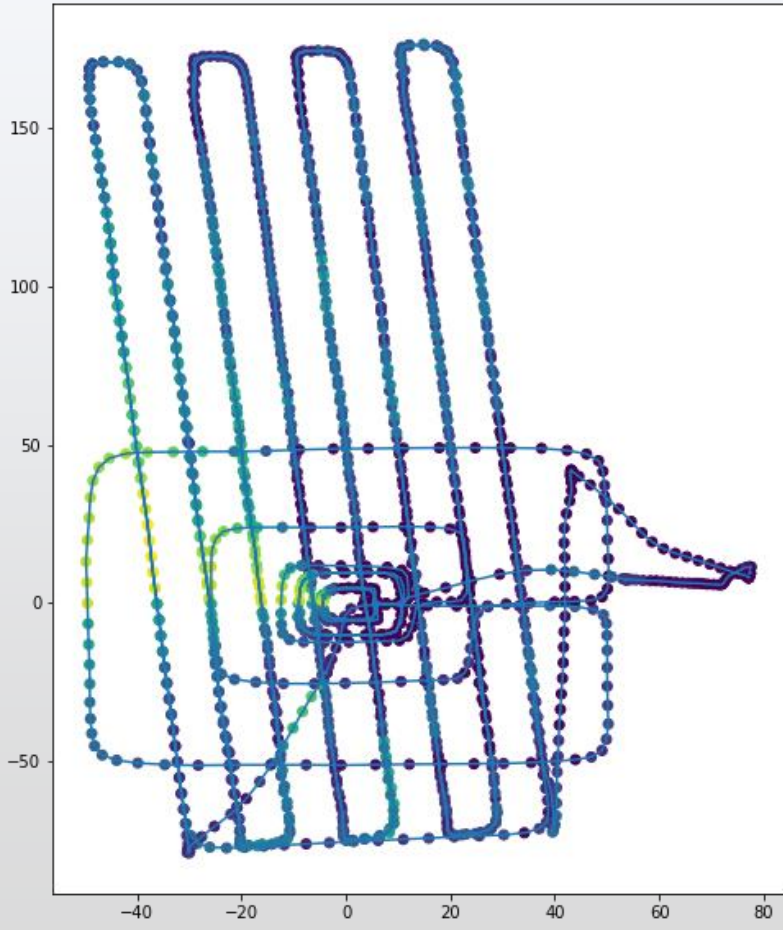
Incorporating our error model into SLAM



Antennas with > 1 Meter Error



Antennas with > 5 Meter Error



Acknowledgements



Future Demos/Collaborators?

- Our relative pose estimation system is becoming increasingly mature.
- If you have other radiological search demos you think might be useful, please reach out!

Email: fishberg@mit.edu

Publications



Multi-Agent Relative Pose Estimation with UWB and Constrained Communications
Presented at IEEE's IROS'22 Conference in Kyoto Japan.



CORA: Certifiably Correct Range-Aided SLAM
Under review; posted to arXiv February 2023



MURP: Multi-Agent Ultra-Wideband Relative Pose Estimation with Constrained Communications in 3D Environments
Being sent to IEEE's RA-L; Posted to arXiv December 2023

Collaborators



Jonathan Rogers
Georgia Tech



Brian Quiter
Lawrence Berkeley National Laboratory



John Fisher
MIT



Alfred Hero
University of Michigan

Graduate Students Supported



Jonathan P. How
PI/Advisor



Andrew Torgesen
(Graduated 2021)



Andrew Fishberg
Current PhD Student

Come talk to me at **Poster #2**

Questions?

ACKNOWLEDGEMENTS

This material is based upon work supported by the Department of Energy / National Nuclear Security Administration under Award Number(s) DE-NA0003921.

